

Spatially correlated fluctuations and coherence dynamics in photosynthesis

Z. G. Yu,^{1,*} M. A. Berding,¹ and Haobin Wang²

¹Physical Sciences Division, SRI International, 333 Ravenswood Avenue, Menlo Park, California 94025, USA

²Department of Chemistry and Biochemistry, New Mexico State University, Las Cruces, New Mexico 88003, USA

(Received 29 July 2008; published 5 November 2008)

Recent multicolor photon-echo experiments revealed a long-lasting quantum coherence between excitations on the donor and acceptor in photosynthetic systems. Identifying the origin of the quantum coherence is essential to fully understand photosynthesis. Here we present a generic model in which a strong intermolecular steric restoring force in densely packed pigment-protein complexes results in a spatial correlation in conformational (static) variations of chromophores, which in turn induces an effective coupling between high-frequency (dynamic) fluctuations in donor and acceptor. The spatially correlated static and dynamic fluctuations provide a favorable environment to maintain quantum coherence, which can consistently explain the photon-echo measurements.

DOI: 10.1103/PhysRevE.78.050902

PACS number(s): 87.15.hg, 78.47.jf, 82.20.Ln, 87.15.ag

Quantum mechanics suggests that any particle can behave like a wave [1]. Such a wavelike behavior or quantum coherence, however, is vulnerable to scatterings and fluctuations and is rarely observed in biological systems, where both conformational variations and high-frequency fluctuations are strong. It is thus widely believed that biological processes can be adequately described by deterministic classical motions. This conventional view is challenged by recent multicolor photon-echo measurements, where a surprisingly long-lasting coherence in photosynthesis [2,3], one of the most important processes to living organisms, was observed. Coherent energy transfer in photosynthesis has profound implications in energy conversion and transportation in biological systems. In these experiments, the off-diagonal density-matrix elements, which measure the quantum coherence between excitations on donor and acceptor chromophores in photosynthetic bacteria, were found to decay much slower than dephasing of the excitations on the donor [3]. To fit the experimental data, a correlation between fluctuations in the donor and acceptor was imposed [3]. The mechanism leading to such a correlation and how it affects the quantum coherence, however, remain unclear. In addition, it was assumed in the fitting that a high-frequency vibrational mode couples to the donor but not the acceptor, which is unusual and hard to justify. Existing theories on energy transfer with multiple chromophores usually assume an independent environment associated with each chromophore [4–7] and do not explain the experiments. On the other hand, spatially correlated disorder and fluctuations were invoked to understand incoherent processes such as electrical transport in polymer films [8] and fluorescent resonant energy transfer in one-dimensional polyproline peptides [9]. In this Rapid Communication we present a unified theory to account for spatially correlated conformational (static) variations and high-frequency (dynamic) fluctuations in densely packed pigment-protein complexes. The calculated photon-echo signals based on this generic theory display a long-lasting coherence, as observed in the experiments.

The reaction center (RC) of the photosynthetic bacteria studied in the experiments consists of six planar chromophores in close proximity (5–10 Å) [10]. These chromophores exhibit two kinds of local environmental fluctuations: Slow-varying conformational variations, in particular, deviations in orientations of the planar chromophores from equilibrium, as shown in large-scale molecular dynamics of photosynthetic proteins [11], and high-frequency vibrations or rotations with respect to the averaged geometry of the chromophores. To understand the impact of such a dense packing of chromophores, as a generic prototype, we carry out first-principles calculations [12] of a system comprising two planar benzene molecules with a relative angle, Θ , separated by a distance, d . We see from Fig. 1 that the total energy of the system can be well-described by $\Delta E = \frac{K}{2}\Theta^2$ and that the intermolecular elastic constant K increases quickly as d becomes small (dense packing). Compared to benzene, a same tilt angle in larger molecules, as those in the RC,

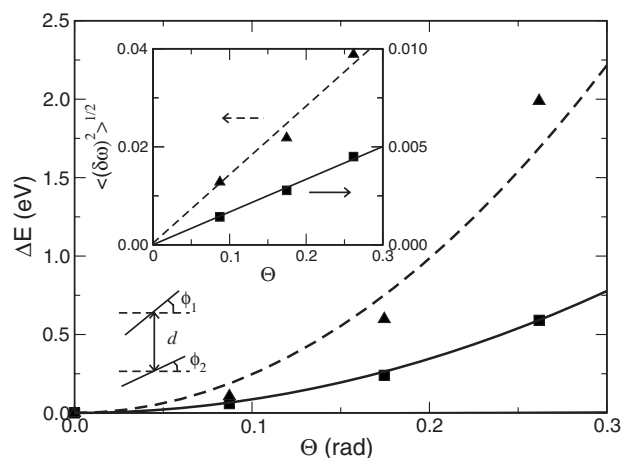


FIG. 1. Total energy of two benzene molecules, represented by the two solid bars in the schematic drawing, as a function of Θ with $d=2.55$ Å (squares) and $d=1.85$ Å (triangles). φ_1 (φ_2) is the orientation change of the upper (lower) benzene molecule from its equilibrium (dashed bars), around the C_2' axis between 1,4 C atoms of benzene, and $\Theta=|\varphi_1-\varphi_2|$. Solid and dashed lines delineate $\Delta E = 8.634\Theta^2$ and $24.62\Theta^2$, respectively. The inset shows $\sqrt{\langle(\delta\omega)^2\rangle}$ as a function of Θ , where the straight lines are plotted to guide the eye.

*zhi-gang.yu@sri.com

corresponds to a longer atomic displacement and the steric energy is significant even at relatively large intermolecular distances. These results suggest the following general Hamiltonian for the conformational variations:

$$\mathcal{H}_C = \sum_{(i,j)} \frac{K}{2} (\phi_i - \phi_j)^2 + \frac{s}{2} \sum_i \phi_i^2, \quad (1)$$

where the chromophores are placed in a cubic lattice (with a lattice constant a) and ϕ_i represents the orientation variation of the chromophore on site i . A possible intramolecular steric energy with s being the corresponding elastic constants is included for completeness. Using the Fourier transform, $\phi_i = \frac{1}{N} \sum_{\mathbf{q}} \Phi(\mathbf{q}) e^{i\mathbf{q} \cdot \mathbf{r}_i}$, where N is the total number of sites in the cubic lattice, and applying the equipartition law $N^{-1} \langle |\Phi(\mathbf{q})|^2 (K\mathbf{q}^2 a^2 + s^2)^{-1} \rangle = k_B T / 2$, where k_B is the Boltzmann constant and T is the temperature, we have [8]

$$\langle \phi_i \phi_j \rangle \equiv \langle \phi_i^2 \rangle \zeta = \langle \phi_i^2 \rangle \frac{a}{r} e^{-\alpha r/a}, \quad (2)$$

where $r = |\mathbf{r}| = |\mathbf{r}_i - \mathbf{r}_j|$, $\alpha = \sqrt{s/K}$, and $\langle \phi_i^2 \rangle = k_B T / 4\pi K$. This expression indicates that conformational variations in densely packed chromophores, where $K \gg s$ and $\alpha \ll 1$, are not independent but similar in magnitude when they are in proximity. The factor ζ measures the correlation strength of the conformational (static) variations. The variance of the relative conformational variation between two chromophores is $\langle [\phi_i - \phi_j]^2 \rangle = 2\langle \phi_i^2 \rangle (1 - \zeta)$, which can be much smaller than that of individual chromophores, $\langle \phi_i^2 \rangle$.

These spatially correlated conformational variations also affect the high-frequency fluctuations. A finite orientation change ϕ_i in a chromophore would cause a shift in the origin of the high-frequency fluctuations, x_i^0 , which is generally proportional to ϕ_i (small ϕ approximation), $x_i^0 = \lambda \phi_i$. To see this effect clearly, we assume that the dynamic fluctuations $x_i(t)$ in two chromophores ($i=1,2$) contain a signal mode with the same frequency, ω ; the Hamiltonian of the fluctuations reads

$$\mathcal{H}_R = \frac{1}{2} \sum_{i=1,2} [p_i^2 + \omega^2 (x_i - \lambda \phi_i)^2], \quad (3)$$

where p_i are the corresponding momenta of x_i . We can obtain an effective Hamiltonian for the fluctuations by integrating out ϕ_k in the partition function, $Z = \int \prod_i \mathcal{D}p_i \mathcal{D}x_i \times \int \prod_k \mathcal{D}\phi_k e^{-(\mathcal{H}_C + \mathcal{H}_R)/k_B T} = \int \prod_i \mathcal{D}p_i \mathcal{D}x_i e^{-\mathcal{H}_{eff}/k_B T}$, where $\int \mathcal{D}$ represents functional integrations, and

$$\mathcal{H}_{eff} = \sum_i \frac{1}{2} (p_i^2 + \omega^2 x_i^2) - \frac{\omega^4 \lambda^2 x_1 x_2 a}{4\pi K r} e^{-\alpha r/a}, \quad (4)$$

which has two normal modes, $x_{\pm} = (x_1 \pm x_2) / \sqrt{2}$, with corresponding frequencies

$$\omega_{\pm}^2 = \omega^2 \left(1 \mp \frac{\lambda^2 \omega^2 a}{4\pi K r} e^{-\alpha r/a} \right) \equiv \omega^2 (1 \mp \xi). \quad (5)$$

The frequency-splitting parameter $\xi \propto \zeta$. To verify that Eqs. (3) and (4) adequately capture the physics, we analyze the vibrational spectrum of the two-benzene system. To avoid ambiguity we focus on the C-H stretch mode, which has a

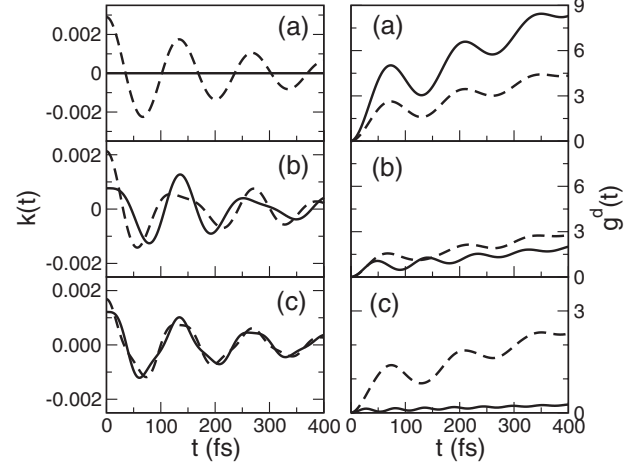


FIG. 2. Temporal correlation functions (left panels) and dynamic dephasing functions (right panels) for different dynamic correlation strengths (ξ). Solid and dashed lines are $k_{12}(t)$ and $k_{11}(t)$ in the left panels, and $\bar{g}_{+-}^d(t)$ and $\bar{g}_{++}^d(t)$ in the right panels. Panels (a)–(c) correspond to $\xi=0, 0.36$, and 0.72 , respectively. The in-phase frequency is fixed, $\hbar\omega_+ = 250 \text{ cm}^{-1}$, $\hbar\gamma = 40 \text{ cm}^{-1}$, $c_1 = c_2 = 2.6 (\text{cm}^{-1})^{1/2} \text{ fs}^{-1}$, $\cos\theta = 0.92$, and $T = 77 \text{ K}$. These values are consistent with those used in Ref. [3].

single peak at ω_0 from the first-principles calculations. In the two-benzene system, the mode split into multiple peaks at ω_i . According to Eq. (5), the averaged frequency splitting, $(\delta\omega)^2 \equiv [(\omega_i^2/\omega_0^2) - 1]^2 = \xi^2 \propto \langle \phi_1 \phi_2 \rangle^2 \sim \Theta^2$, or $\sqrt{(\delta\omega)^2} \sim \Theta$, as confirmed in Fig. 1. Hence the spatially correlated conformational variations induce an effective coupling between the dynamic fluctuations in the two chromophores, which creates an in-phase mode x_+ with a lower frequency and an out-of-phase mode x_- with a higher frequency.

To gain insight into the correlated dynamic fluctuations, it is instructive to examine the temporal correlation between x_i and x_j , $k_{ij}(\tau) \equiv x_i(t)x_j(t-\tau)$. To evaluate $k_{ij}(\tau)$, we notice that the new normal modes x_{\pm} can be generally described by damped oscillators, which obey the following Langevin equation, $\frac{d^2 x_{\pm}}{dt^2} + \omega_{\pm}^2 x_{\pm} - \gamma \frac{dx_{\pm}}{dt} = F(t)$, where γ is the damping factor and $F(t)$ is a random force. According to the fluctuation-dissipation theorem (FDT), $\mathcal{X}_{\pm}^2(\omega) = 2\gamma k_B T / [(\omega^2 - \omega_{\pm}^2)^2 + \gamma^2 \omega^2]$ with $\mathcal{X}_{\pm}(\omega) = \int_{-\infty}^{+\infty} dt e^{i\omega t} x_{\pm}(t)$. The temporal correlation functions of the normal modes are $K_{\pm}(\tau) \equiv x_{\pm}(t)x_{\pm}(t-\tau) = \int_{-\infty}^{+\infty} \mathcal{X}_{\pm}^2(\omega) e^{i\omega\tau} d\omega$,

$$K_{\pm}(\tau) = \frac{k_B T e^{-\gamma|\tau|/2}}{\omega_{\pm}^2} \left(\cos \omega'_{\pm} \tau + \frac{\gamma}{2\omega'_{\pm}} \sin \omega'_{\pm} \tau \right),$$

where $\omega'_{\pm} = \omega_{\pm}^2 - \gamma^2/4$. Here, for clarity and tractability, the classical form of the FDT is adopted. The more subtle quantum FDT does not qualitatively modify the results [13]. Since x_{\pm} are orthogonal, we have $k_{11}(\tau) = k_{22}(\tau) = \frac{1}{2}[K_+(\tau) + K_-(\tau)]$ and $k_{12}(\tau) = k_{21}(\tau) = \frac{1}{2}[K_+(\tau) - K_-(\tau)]$. Figure 2 shows $k_{11}(t)$ and $k_{12}(t)$ for various dynamic correlation strengths. In the absence of spatial correlation, $\xi=0$, the two dynamic fluctuations x_1 and x_2 are independent, and there is no temporal correlation between them. With increase of ξ , the temporal correlation between x_1 and x_2 becomes more signifi-

cant. At $\xi=0.72$, $k_{12}(t)$ and $k_{11}(t)$ are almost the same, indicating that x_1 and x_2 are largely synchronized.

The static and dynamic fluctuations will cause the energy of an excitation (exciton) on chromophore i to vary around its average value, E_i^0 , $\delta E_i(t) = \delta E_i^s + \delta E_i^d = \nu_i \phi_i + c_i x_i(t)$, where ν_i and c_i are the coupling constants between the exciton and the local static and dynamic fluctuations, which will lead to dephasing of the exciton and broaden the absorption line. The line-shape function in the time domain is defined by [16]

$$J_{ii}(t) = e^{-(i/\hbar)E_i^0 t} \langle e^{-(i/\hbar) \int_0^t dt' \delta E_i(t')} \rangle \equiv e^{-(i/\hbar)E_i^0 t - g_{ii}(t)}, \quad (6)$$

where $g_{ii}(t) = g_{ii}^s(t) + g_{ii}^d(t)$ consists of contributions from both static and dynamic fluctuations. A large $g_{ii}(t)$ means a fast dephasing of the excitation in chromophore i . By using the relation $\langle e^{iX(t)} \rangle = \exp(-\frac{1}{2}X^2(t))$, $g_{ij}(t)$ can be written as

$$g_{ij}^s(t) = \frac{1}{2\hbar^2} \nu_i \nu_j \langle \phi_i \phi_j \rangle t^2 \equiv \frac{1}{2} \Delta_{ij} t^2,$$

$$g_{ij}^d(t) = \frac{c_i c_j}{\hbar^2} \int_0^t d\tau (t - \tau) k_{ij}(\tau),$$

which can be worked out analytically,

$$\Delta_{ii} = \frac{\nu_i^2 k_B T}{4\pi\hbar^2 K}, \quad \Delta_{12} = \frac{\nu_1 \nu_2 \zeta k_B T}{4\pi\hbar^2 K},$$

$$g_{ii}^d(t) = \frac{k_B T c_i^2}{2\hbar^2} \left[\frac{G(\omega_+, t)}{\omega_+^4} + \frac{G(\omega_-, t)}{\omega_-^4} \right],$$

$$g_{12}^d(t) = \frac{k_B T c_1 c_2}{2\hbar^2} \left[\frac{G(\omega_+, t)}{\omega_+^4} - \frac{G(\omega_-, t)}{\omega_-^4} \right],$$

$$G(\omega, t) = \gamma |t| - e^{-\gamma |t|/2} \left[1 + \left(\frac{\gamma}{2\omega'} \right)^2 \right]^{1/2} \cos(\omega' t + \theta - \theta'), + 1,$$

where $\omega'^2 = \omega^2 - \gamma^2/4$, $\theta = \tan^{-1} \gamma \omega' / [(\gamma/2)^2 - \omega'^2]$, and $\theta' = \tan^{-1} \gamma/2\omega'$.

To study the coherence in exciton transfer from donor to acceptor, we notice that only the difference between the donor and acceptor environments is important to the transfer and consider the Hamiltonian, $H = H_e + H_f$. The excitonic Hamiltonian is

$$H_e = E(a_1^\dagger a_1 - a_2^\dagger a_2) + U(a_1^\dagger a_2 + a_2^\dagger a_1), \quad (7)$$

where a_i^\dagger (a_i) creates (annihilates) an exciton on the donor ($i=1$) or acceptor ($i=2$), $E = (E_1^0 - E_2^0)/2$, and U is the exciton hopping between the donor and acceptor. The interaction between the exciton and the fluctuating environments is

$$H_f = \frac{1}{2}(c_1 x_1 - c_2 x_2 + \nu_1 \phi_1 - \nu_2 \phi_2)(a_1^\dagger a_1 - a_2^\dagger a_2). \quad (8)$$

Hamiltonian H has the same form as the spin-boson model [14] widely used to study energy transfer in photosynthesis [4–7, 18, 19], except that its environmental variables are now spatially correlated. When the exciton hopping U is not negligible, it is more appropriate to study the coherence in the

eigenstate basis of H_e . $H_e = \epsilon(a_1^\dagger a_+ - a_1^\dagger a_-)$ with $\epsilon = \sqrt{E^2 + U^2}$. The dephasing functions for the eigenstates $|\pm\rangle$ can be similarly defined as in Eq. (6) and expressed in terms of g_{ij} , $g_{++}(t) = c^4 g_{11}(t) + s^4 g_{22}(t) + 2s^2 c^2 g_{12}(t)$, $g_{--}(t) = c^4 g_{22}(t) + s^4 g_{11}(t) + 2s^2 c^2 g_{12}(t)$, and $g_{+-}(t) = c^2 s^2 [g_{11}(t) + g_{22}(t)] + (s^4 + c^4) g_{12}(t)$, where $c \equiv \cos(\theta/2)$, $s \equiv \sin(\theta/2)$, and $\theta = -\tan^{-1}(U/E)$.

The dynamics of the exciton density matrix can be obtained by solving the Liouville equation in the interaction representation, $\frac{d\rho^*(t)}{dt} = \frac{i}{\hbar}[\rho^*(t), H_f]$, with $\rho(t) = e^{-iH_e t/\hbar} \rho^*(t) e^{iH_e t/\hbar}$. Explicitly, for the off-diagonal ρ_{+-}^* ,

$$\frac{d\rho_{+-}^*}{dt} = \frac{i}{\hbar} \sum_m [(+|\rho^*|m)(m|H_f(t)|-) e^{-(i/\hbar)(E_m - E_-)t} - (+|H_f(t)|m)(m|\rho^*|-) e^{-(i/\hbar)(E_+ - E_m)t}].$$

We adopt the adiabatic approximation [15], where only the terms with $E_m = E_-$ or $E_m = E_+$ should be retained, since all the others, because of their fast varying exponential coefficients, give a negligible contribution. The simplified equation has a general solution $\rho_{+-}^* = \rho_{+-}^*(0) \exp i \int_0^t \omega_{+-}(t') dt$, where $\omega_{+-}(t) = [(+|H_f(t)|+) - (-|H_f(t)|-)]/\hbar = \cos \theta [\sqrt{2}(c_+ x_+ + c_- x_-) + \nu_1 \phi_1 - \nu_2 \phi_2]/\hbar$ and $c_{\pm} = (c_1 \mp c_2)/2$. The coherence dynamics in exciton transfer can be quantified by the following function:

$$\tilde{J}_{+-}(t) = e^{-(i/\hbar)(E_+ - E_-)t} \left\langle \frac{\rho_{+-}^*(t)}{\rho_{+-}^*(0)} \right\rangle = e^{-(i/\hbar)2\epsilon t - \tilde{g}_{+-}(t)}, \quad (9)$$

where $\tilde{g}_{+-}(t) = \tilde{g}_{+-}^s(t) + \tilde{g}_{+-}^d(t)$, and

$$\tilde{g}_{+-}^s(t) = \frac{\cos^2 \theta}{2} (\Delta_{11} + \Delta_{22} - 2\Delta_{12}) t^2,$$

$$\tilde{g}_{+-}^d(t) = \frac{2 \cos^2 \theta k_B T}{\hbar^2} \left[\frac{c_+^2 G(\omega_+, t)}{\omega_+^4} + \frac{c_-^2 G(\omega_-, t)}{\omega_-^4} \right].$$

$\tilde{g}_{+-}(t)$ and $g_{ij}(t)$ are related, $\tilde{g}_{+-}(t) = g_{++}(t) + g_{--}(t) - 2g_{+-}(t) = \cos^2 \theta [g_{11}(t) + g_{22}(t) - 2g_{12}(t)]$. The inhomogeneous broadening in \tilde{J}_{+-} , caused by the static fluctuations, is $1/T_2^* = \cos \theta \sqrt{\Delta_{11} + \Delta_{22} - 2\Delta_{12}}$. It is clear that as the correlation between static fluctuations, Δ_{12} , increases, the inhomogeneous broadening will be reduced. We compare in Fig. 2 $\tilde{g}_{+-}^d(t)$ with $g_{++}^d(t)$, the dynamic dephasing function for the eigenstate $|+\rangle$ (approximate donor state), for different correlation strengths ξ . In the absence of spatial correlation, $\tilde{g}_{+-}^d(t)$ is much larger than $g_{++}^d(t)$, indicating a much faster dephasing for the off-diagonal elements of the exciton density matrix than the dephasing for excitons on the donor or acceptor. As the correlation increases, $\tilde{g}_{+-}^d(t)$ is considerably reduced, while $g_{++}^d(t)$ changes little. At $\xi=0.72$, $\tilde{g}_{+-}^d(t)$ becomes much smaller than $g_{++}^d(t)$, suggesting a long-lasting coherence of the off-diagonal elements. In the overdamped regime, i.e., $G(\omega, t) \approx \gamma |t|$ the dynamic fluctuations give rise to a homogeneous broadening, $\tilde{g}_{+-}^d(t) = |t|/T_2$ with $1/T_2 = 2 \cos^2 \theta k_B T \gamma (c_+^2/\omega_+^4 + c_-^2/\omega_-^4)/\hbar^2$ for exciton transfer between the donor and acceptor. T_2 (T_2^*) is the intrinsic (extrinsic) dephasing time for the exciton transfer from donor to

acceptor. The intrinsic (extrinsic) dephasing time of the exciton on the donor or acceptor, T_3 (T_3^*), can be similarly defined via $g_{++}(t)$, with $1/T_3^* = \sqrt{c^4\Delta_{11} + s^4\Delta_{22} + 2s^2c^2\Delta_{12}}$, and $1/T_3 = k_B T (c_1^2 c^4 + c_2^2 s^4 + 2c_1 c_2 c^2 s^2) \gamma (\omega_+^{-4} + \omega_-^{-4}) / 2\hbar^2$. While T_2 and T_2^* are always shorter than T_3 and T_3^* in the absence of the spatial correlation, a significant spatial correlation can reverse the order and results in long T_2 and T_2^* .

In the multicolor photon-echo experiments, three laser pulses were applied to the sample at times 0, t_1 , and t_2 , respectively. In a two-dimensional map of the echo signals as a function of t_1 and t_2 , an oscillatory behavior was observed along the t_2 axis but not along the t_1 axis. To understand these experiments, we compute the echo signals via [3,16–19] $S(t_1, t_2) \sim \int_0^\infty dt e^{-2f(t_1, t_2, t)}$, where $f(t_1, t_2, t) = g_{++}(t_1 + t_2) - g_{+-}(t_1 + t_2 + t) + g_{+-}(t_1) + g_{+-}(t) - g_{+-}(t_2) + g_{--}(t_2 + t)$. The left panels in Fig. 3 show $S(t_1, t_2)$ as a function of t_2 with a fixed $t_1 = 30$ fs, as in Fig. 3 of Ref. [3]. When the correlation is absent, the echo signal for $t_2 \geq 100$ fs is a rapid monotonic decay. Only when the correlations are strong enough does an oscillatory behavior similar to the measurements appear. The oscillatory behavior is a direct consequence of the long-lasting coherence of the off-diagonal elements in the exciton density matrix, caused by the spatially correlated static and dynamic fluctuations. The right panels show $S(t_1, t_2)$ as a function of t_1 with a fixed $t_2 = 100$ fs. No oscillatory behavior is present even with strongly correlated fluctuations, which is consistent with experiment. The reason is that by varying t_1 , the echo signal mainly reflects the dephasing of the exciton on the donor, $g_{++}(t)$, which remains strong as the correlation strengths increase, as shown in Fig. 2. For $(\xi, \zeta) = (0.72, 0.90)$, the photon-echo signals, plotted in a color map as a function of t_1 and t_2 , resemble those from experiment, although a quantitative explanation of experiment requires further studies [13].

In summary, we have developed a generic theory that identifies the origin of the spatially correlated conformational variations and high-frequency fluctuations in densely packed

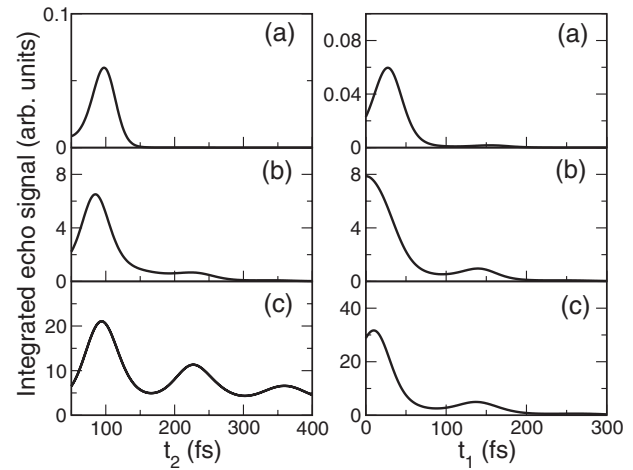


FIG. 3. Photon-echo signal as a function of t_2 with a fixed $t_1 = 30$ fs (left panels) and as a function of t_1 with a fixed $t_2 = 100$ fs (right panels) for different static and dynamic correlation strengths, ζ and ξ . Panels (a)–(c) correspond to $(\xi, \zeta) = (0, 0)$, $(0.36, 0.45)$, and $(0.72, 0.90)$, respectively. Parameters are $\hbar\sqrt{\Delta_{11}} = \hbar\sqrt{\Delta_{22}} = 20$ cm $^{-1}$. Other parameters are the same as in Fig. 2.

chromophores in photosynthetic bacteria and elucidates their effects on coherence dynamics. Further studies, including molecular dynamics and electronic structures of the photosynthetic RC, are needed to quantitatively describe the quantum coherence and photon-echo experiments. It is fascinating that the macroscopic and primitive elastic energy, when acting collectively, can provide a favorable environment to protect the microscopic and delicate quantum coherence in strongly fluctuating biological systems.

This work was supported by the U.S. Army Research Office under Contract No. W911NF05C0070. H.W. also acknowledges support from the National Science Foundation Grant No. CHE-0348956.

- [1] See, e.g., L. D. Landau and E. M. Lifshitz, *Quantum Mechanics*, 3rd ed. (Pergamon, Oxford, 1977).
- [2] G. S. Engel, T. R. Calhoun, E. L. Read, T. K. Ahn, T. Mancal, Y. C. Cheng, R. E. Blankenship, and G. R. Fleming, *Nature* (London) **446**, 782 (2007).
- [3] H. Lee, Y. C. Cheng, and G. R. Fleming, *Science* **316**, 1462 (2007).
- [4] R. E. Blankenship, *Molecular Mechanisms of Photosynthesis* (Blackwell Science, Oxford, 2002).
- [5] R. van Grondelle and V. I. Novoderezhkin, *Phys. Chem. Chem. Phys.* **8**, 793 (2006).
- [6] O. Kühn, V. Sundström, and T. Pullerits, *Chem. Phys.* **275**, 15 (2002).
- [7] S. Jang, M. D. Newton, and R. J. Silbey, *Phys. Rev. Lett.* **92**, 218301 (2004).
- [8] Z. G. Yu, D. L. Smith, A. Saxena, R. L. Martin, and A. R. Bishop, *Phys. Rev. Lett.* **84**, 721 (2000); *Phys. Rev. B* **63**, 085202 (2001).
- [9] Z. G. Yu, *J. Chem. Phys.* **127**, 221101 (2007).
- [10] U. Ermler, G. Fritzsh, S. K. Buchanan, and H. Michael, *Structure* (London) **2**, 925 (1994).
- [11] D. E. Chandler, J. Hsin, C. B. Harrison, J. Gumbart, and K. Schulten, *Biophys. J.* **95**, 2822 (2008).
- [12] Results were obtained by using Dmol 3 [B. Delley, *J. Chem. Phys.* **92**, 508 (1990)] from Accelrys, Inc. with the DNP basis sets and PW91 functional in the general gradient approximation. The vibrational modes for different geometries were obtained by diagonalizing the mass-weighted force constant matrix.
- [13] Z. G. Yu, M. A. Berding, and H. Wang (unpublished).
- [14] A. J. Leggett, S. Chakravarty, A. T. Dorsey, M. P. A. Fisher, A. Garg, and W. Zwerger, *Rev. Mod. Phys.* **59**, 1 (1987).
- [15] The observed long-lasting coherence suggests that the incoherent exciton transfer is insignificant within a few hundred femtoseconds after an exciton is created on the donor.
- [16] S. Mukamel, *Principles of Nonlinear Optical Spectroscopy* (Oxford University Press, New York, 1995).
- [17] T. Meier, V. Chernyak, and S. Mukamel, *J. Chem. Phys.* **107**, 8759 (1997).
- [18] M. Yang and G. R. Fleming, *J. Chem. Phys.* **110**, 2983 (1999).
- [19] T. Mancal and G. R. Fleming, *J. Chem. Phys.* **121**, 10556 (2004).